BEHAVIOR OF GAS BUBBLES IN A CONCENTRIC CYLINDRICAL AIRLIFT COLUMN

Keun Ho Choi* and Won Kook Lee

*Department of Chemical Engineering, Taejon National University of Technology,
305, Samsung-dong, Dong-gu, Taejon 300-172, Korea
Department of Chemical Engineering, Korea Advanced Institute of Science and Technology,
373-1, Kusong-dong, Yusung-gu, Taejon 305-701, Korea

Abstract—Using a light transmission optical probe, the effect of superficial gas velocity on bubble properties(bubble size, bubble rising velocity, bubble frequency and local gas holdup) at axial and radial positions was determined in the riser and the downcomer of a concentric cylindrical airlift reactor. The vertical bubble length, the bubble rising velocity and the bubble frequency at axis in the riser increased with increasing superficial gas velocity and the bed height. The radial distribution of the local gas holdup, vertical bubble length and bubble frequency in the riser and the downcomer were found to be non-uniform. The profiles of the local gas holdup, vertical bubble length and bubble rising velocity in the riser were shown as parabolic shapes. The local gas holdup, the vertical bubble length and the bubble frequency in the downcomer changed with superficial gas velocity and the distance from the top of the draft tube.

INTRODUCTION

Fundamentally the several demands are essentially valid for any bioreactors with heterogeneous gas-liquid-phases. Among these, oxygen transfer, mixing and heat removal are three of the chief problems involved in developing a fermentation process. Using the design principle of the airlift reactor, effective oxygen transfer rates, mixing rates and heat transfer rates can be attained at power costs competitive or lower than conventional fermenters [1].

The configurations of the airlift reactor are a bubble column with external loop and a bubble column divided into two sections by a internal baffle. As a gas is sparged into one section, the density difference between the bubbly liquids in the sparged section(riser) and the unsparged section(downcomer) occurs and induces a definitely directed liquid circulation.

Despite many advantages, the commercial application of airlift reactors in biotechnology is still quite limited due to insufficient data available for their design [2]. Bubble size, bubble rising velocity, bubble size distribution and bubble rising velocity profiles

have a direct bearing on the performance of airlift reactors. These parameters control the gas holdup, gas-liquid interfacial areas, and the rate of oxygen transfer. Therefore, it is expected that these properties supply important data for the design of bioreactors. Although many experimental studies of bubble dynamics have been carried out in airlift reactors [3-15], the main difficulty in modeling of the reactor is the lack of information on the hydrodynamics of the reactor.

On the other hand, direct determination of the interfacial area by the usual chemical method is inadequate for biological systems because toxic conditions produced by the method are detrimental to micro-organisms. During cultivation, only physical methods can be used to determine the interfacial area. Recently, for measuring the bubble sizes or the interfacial area, the electrical and optical probes have been more widely used than the photographic method. Using the electrical probe method or the optical probe method, it is possible to measure the rising velocity of bubbles and their sizes simultaneously, even though the gas flow rate is very high or the columns are opaque.

The aim of present investigation is to collect more basic data of bubble properties in the riser and the

---

*To whom all correspondence should be addressed.

Table 1. Dimensions of the experimental apparatus and experimental conditions

Concentric cylinder airlift reactor	
Outer column i.d.	0.238 m
Draft tube i.d.	0.146 m
Draft tube length	1.10 m
Gas-liquid separator	0.4×0.4×0.2 m
Distance of draft tube from bottom	0.05 m
Gas phase and liquid phase	: Air and tap water
Superficial gas velocity	: 0.02-0.20 m/s
Superficial liquid velocity	: 0 m/s
Aerated liquid height	: 1.55 m
Measuring points for bubble properties	

| Section	Height(H)	Radial position(r)
Downcomer	0.1, 0.3, 0.5, 0.7, 0.9, 1.1	0.087, 0.095, 0.103, 0.111
Riser	0.4, 0.6, 0.8, 1.0	0, 0.02, 0.04, 0.06, 0.068

downcomer for a better understanding of the interrelation between fluid dynamics and mass transfer phenomena in airlift reactors. In this investigation, using a light transmission optical probe, variation of bubble properties(bubble size, bubble rising velocity, bubble frequency and local gas holdup) with the superficial gas velocity, bed height and dimensionless radial position was measured in a concentric cylindrical airlift reactor.

EXPERIMENTAL

Experimental were carried out in a concentric cylindrical airlift vessel. The dimensions of various parts of the vessel and experimental conditions are listed in Table 1. The airlift reactor were operated in the semi-batch mode of operation. The details of the experimental setup and experimental procedures are described in previous publication [16].

For measurement of bubble properties, a light transmission probe were used in this work. A sketch of the probe system was shown in Fig. 1. The light transmission optical probe was consisted of two pairs of optical fibers of 0.5 mm diameter; one pair were used as a light projector, and the other at the opposite side were as a receiver of the light transmitted across the probe spacing.

The light source was a Helium-Neon laser(Spectra-Physics, model 102) and the detector is a photoelectric cell(Kodenshi Corp., ST-1KLA Photo transistor). The optical probe gives optical signals corresponding to phase changes due to the passage of a bubble through the probe tip. The optical signal was conver-
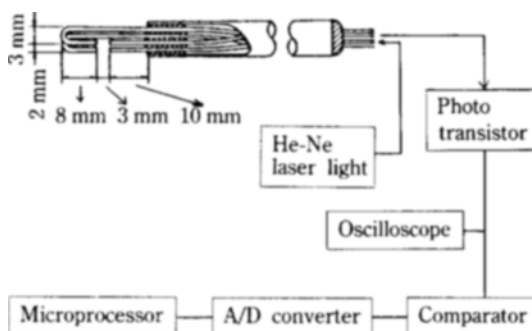
Fig. 1. Schematic diagram of optical probe system.
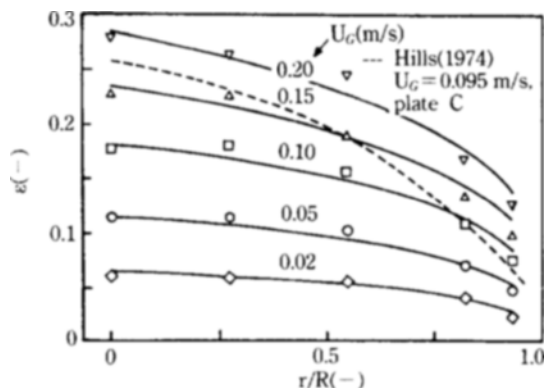
Fig. 2. Radial distribution of local gas holdup in riser as a function of superficial gas velocity(H=0.6 m), —; Eq.(1).

ted to the electrical signal by a comparator circuit. After the comparator, the signal was converted to digital form by A/D converter(Analog Design Laboratory Co., ADL-1000M) with sampling periods of 200 μs and 400 μs for the riser and the downcomer, respectively. Then the two possible values of the cell current are, unity if the probe tip is in the liquid phase, and zero if it is in the gas. The signals were fed to an online microprocessor for calculating the bubble properties. The details of calculation method of bubble properties are described in previous publication [16].

RESULT AND DISCUSSION

1. Bubble Properties in Riser

The radial distribution of the local gas holdup is presented in Fig. 2 as a function of the dimensionless radial position. Fig. 2 shows considerable variation of gas holdup with the radial position. The local gas holdup profiles were parabolic curves. Lippert et al. [4]. had observed similar results in an external-loop airlift
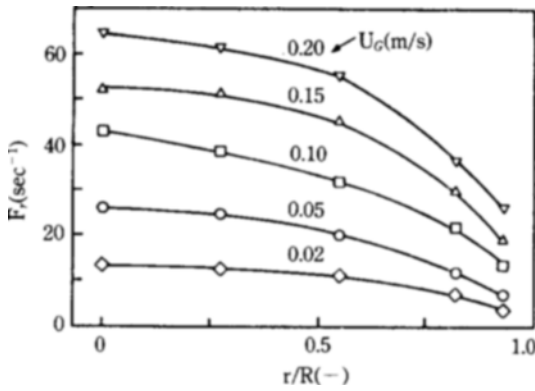
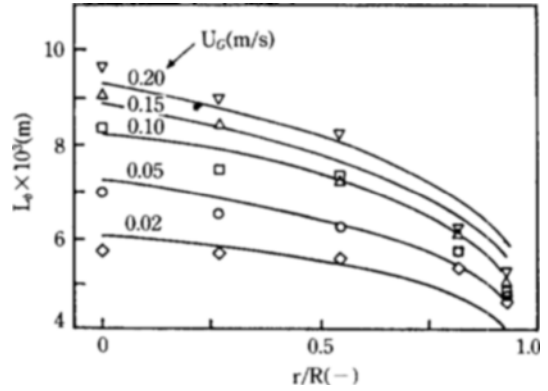Fig. 3. Radial distribution of local bubble frequency in riser as a function of superficial gas velocity(H = 0.6 m).

Fig. 4. Radial distribution of vertical bubble length in riser as a function of superficial gas velocity(H = 0.6 m), —; Eq.(2).

Fig. 5. Radial distribution of local bubble rising velocity in riser as a function of superficial gas velocity(H = 0.8 m), —; Eq.(3).

reactor. Because of wall effect, the bubbles tend to move away from the wall toward a central point as they rise. At specific gas velocity, the highest value of the local gas holdup was observed in center of the draft tube. The gas holdup diminished with an increase in the dimensionless radial position, r/R, and attained low values close to the wall of the tube. In the case of higher gas rates, there was an increasingly sharp central maximum in local gas holdup. The change of local gas holdup according to r/R is a parabolic shape. In present study, the measured gas holdup profile was well fitted by the following equation:

$$\varepsilon = 0.885 U_G^{0.645} H^{0.185}\left(1 - \frac{r}{R}\right)^{0.273} \qquad (1)$$
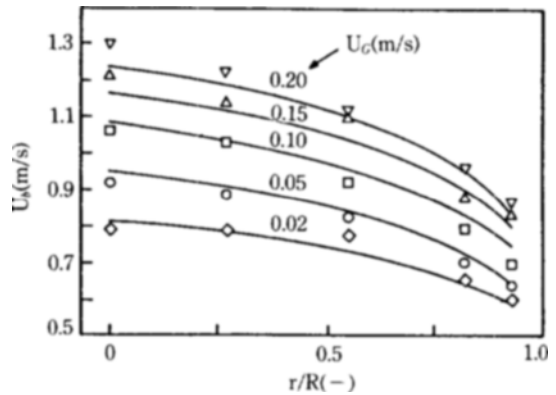
$$(R.C. = 0.995, \ S.D. = 0.0076)$$

Hills [17] also reported the parabolic profiles of the local gas holdup in bubble columns. His gas holdup data are also shown in Fig. 2. In the case of airlift reactor, the circulating liquid flow increases the distance between bubbles and depresses the bubble coalescence. So the radial distribution of the local gas holdup is more uniform in the airlift reactor than the bubble column at same gas velocity. Therefore, airlift reactors are capable of high gas flow rates without formation of slugs. In addition, Serizawa et al. [18] have observed that the radial distribution of the local gas holdup was a saddle shape distribution in the case of bubbly flow for a bubble column. But, in this work, the saddle shape distribution of the local gas holdup was not observed because the liquid circulation is present in airlift reactors.

Bubble frequency is influenced by the gas holdup, bubble size and bubble rising velocity as well as the intensity of liquid turbulence. As shown in Fig. 3, the

bubble frequency at any radial position increased with superficial gas velocity. It is certain that the local gas holdup, bubble rising velocity and the intensity of liquid turbulence increase with increasing gas flow rate. The radial distribution of the bubble frequency in the riser was also a parabolic profile.

Typical radial profiles of the vertical bubble length and bubble rising velocity are shown in Fig. 4 and Fig. 5, respectively. When the superficial gas velocity is low the bubble coalescence is not severe. Therefore, at low gas flow rate($U_G = 0.02 \ ms^{-1}$), the vertical bubble length and bubble rising velocity were almost independent of the radial position. The size and rising velocity of bubbles decreased only in the wall region. With increasing gas flow rates, the profiles of the vertical bubble length and bubble rising velocity showed
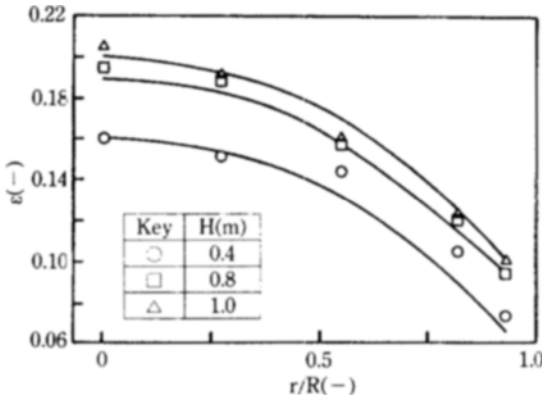
Fig. 6. Radial distribution of local gas holdup in riser as a function of bed height(U_G=0.1 m/s).
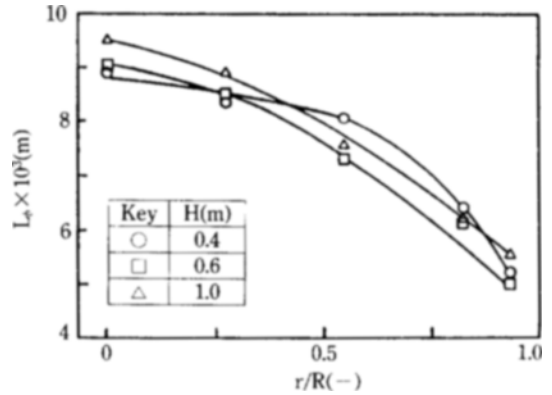

Fig. 7. Radial distribution of local bubble rising velocity in riser as a function of bed height(U_G=0.1 m/s).

the characteristic parabolic shapes, respectively. The highest values of the vertical bubble length and bubble rising velocity were occurring in the center region of the draft tube. The wall effect and uneven distribution of the local gas holdup created by the liquid circulation provoke a higher velocity of the two phase mixture in the center of the draft tube. The gradient of liquid velocity in the radial direction induces a migration of bubbles toward the axis. In the center region of the tube, large bubbles are formed by bubble coalescence resulting in a high concentration of bubbles. Lippert et al. [4] conducted the experiments for the radial distributions of the bubble rising velocity, and mean and Sauter bubble diameters in the riser of an external-loop airlift reactor during culture. They have reported that the local gas holdup and mean bubble diameter varied in the core of the flow approximately like a parabolic profile.

The bubble coalescence and break-up were observed in the riser section. Although the bubble break-up and bubble coalescence increase as the superficial gas velocity increases. The vertical bubble length at the central point was found to increase with an increase in air flow rate because the bubble coalescence rate would tend to overcome bubble break-up rate. Bubbles coalesce at a rate approximately proportional to their collision frequency which is proportional to the square of bubble concentration.

Mercer [3], Popovic and Robinson [10] and Glasgow et al. [6] mentioned that average bubble sizes diminished with increasing aeration rates in the riser of airlift reactors. In contrast to them, other researchers reported an increasing bubble size due to coalescence when the reactor was operated at high aeration rates [5, 7]. This discrepancies may arise from differences between the measuring methods.

The bubble rising velocity strongly depends on the bubble size and the liquid circulation velocity in an airlift reactor. At the central point, both the vertical bubble length and liquid circulation velocity increase as the gas velocity increases. Therefore, Fig. 5 shows that the bubble rising velocity at the central point increases with increasing gas velocity.

Present data for vertical bubble length can be correlated by the following equation:

$$L_b = 0.013 U_G^{0.180} H^{0.091} \left(1 - \frac{r}{R}\right)^{0.172} \qquad (2)$$

$$(R.C. = 0.947, \ S.D. = 0.00048)$$

The measured local bubble rising velocity profile was well fitted by the following equation:

$$U_b = 1.639 U_G^{0.178} H^{0.031} \left(1 - \frac{r}{R}\right)^{0.140} \qquad (3)$$

$$(R.C. = 0.963, \ S.D. = 0.048)$$

Fig. 6 presents the typical radial distribution of the local gas holdup as a function of bed height. The local gas holdup gradually increases with increasing the bed height because of the volume expansion of bubbles due to the decrease of pressure.

The radial profiles of the vertical bubble length and bubble rising velocity as a function of bed height are presented in Fig. 7 and Fig. 8, respectively. At the central point, the vertical bubble length and the bubble rising velocity were increased by an increase in bed height. The results indicate that the two-phase flow does not appears to be fully developed in the riser section. Serizawa et al. [18] reported that a fully-developed flow was attained at H = 30D for bubble flow, whereas in transition and slug flows the entrance length was less than 30D for air-water system. However, in this experiment, the maximum value of the en-
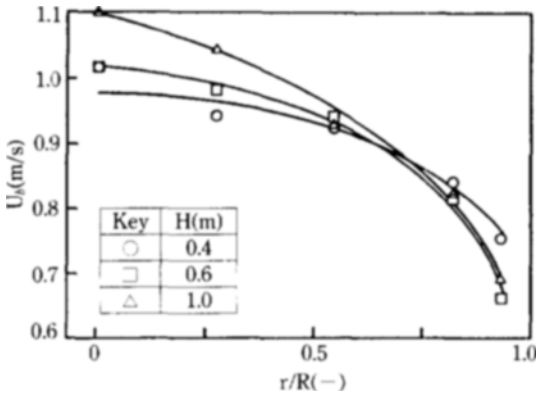
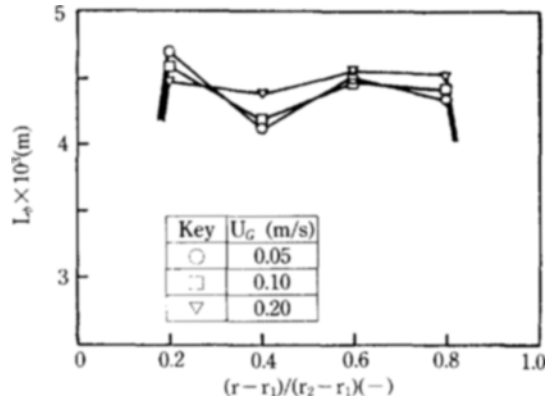**Fig. 8. Radial distribution of vertical bubble length in riser as a function of bed height($U_G=0.15$ m/s).**

Fig. 9. Radial distribution of vertical bubble length in downcomer as a function of superficial gas velocity (Z=0.05 m).

Fig. 10. Effect of superficial gas velocity on cross-sectional average of vertical bubble length in downcomer.

trance length was 7.534 D_D.

At low gas velocities($U_G=0.02$ ms^{-1}), the bubbles ascended in almost straight lines. Since the lateral component of the velocity vector was very small, the bubbles rise without collision each other. Therefore, the bubble size slightly decreased with the bed height due to the continuous breakage of primary bubbles as they rise from the sparger and are exposed to the turbulent flow field [6]. However, at high gas velocity above 0.1 ms^{-1}, the flow oscillations occurred and the bubble coalescence phenomenon becomes more and more important. Fig. 7 shows that the mean vertical bubble length at central point increased with increasing bed height. Ueyama et al. [19] pointed that when U_G was in the range 0.07 to 0.2 ms^{-1}, bubbles began to coalesce because of the increase in gas holdup. Similarly, Fig. 8 shows that the bubble rising velocity at the central point in the riser increases with increasing bed height due to bubble coalescence and developing two-phase flow in the region. Glasgow et al. [6] reported that bubble size distributions in the riser and downcomer regions followed a log-normal distribution function and the distribution gradually shifted towards the small bubble region as the observation moves from the bottom to the top. This discrepancies also may results from differences between the measuring methods. They have used the photographic method for measurement of the bubble size. In the case of the measurement of bubbles which exist in the central region of the vessel or a large gas-feed rate, the photographic method is not suitable for obtaining a true average size of bubbles.

2. Bubble Properties in Downcomer

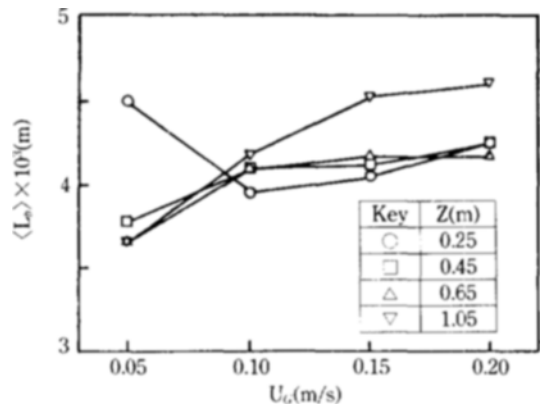The average bubble size in the downcomer is smaller than that in the riser. The forces on a bubble in the downcomer section are the buoyant force and the drag force, acting in opposite directions. The net direction of flow for a large bubble will be upward and that for a small bubble will be downward [15, 20]. The larger bubbles rise near the vessel wall at the same time that bubbles of similar size are being carried downward farther away from the vessel wall. Therefore, there existed a change of bubble sizes in the redial direction and the bubble size reduced towards the lower region of the downcomer [13-15].

Fig. 9 shows the radial distribution of vertical bubble length in the downcomer. The vertical bubble length was slightly great at near the draft tube wall due to the presence of rising coalesced bubbles. Bubble frequency depends on the gas holdup, bubble size and velocity, and fluctuation of liquid velocity. But the

shape of the local bubble frequency profile in the down-comer was also similar to the distribution of the vertical bubble length.

The effect of superficial gas velocity on the cross-sectionally averaged vertical bubble length in the down-comer is shown in Fig. 10. The cross-sectionally averaged vertical bubble length were obtained by graphical integration, using Simpson's rule.

$$\langle L_h \rangle = \frac{\int_{r_1}^{r_2} n_b L_b r \ dr}{\int_{r_1}^{r_2} n_b r \ dr} \tag{4}$$

For the middle and lower sections of the downcomer, the cross-sectionally averaged vertical bubble length increased with increasing gas velocity. The entrained bubble size into the downcomer strongly depends on the circulation liquid velocity. A bubble was entrained into the downcomer when the liquid velocity was higher than the terminal velocity of a bubble. The circulation liquid velocity increased as superficial gas velocity increased. However, the effect of superficial gas velocity on the vertical bubble length in the upper section of the downcomer, at $Z = 0.25$ m, showed a different trend. The measured cross-sectional average of the vertical bubble length for $Z = 0.25$ decreased until $U_G = 0.1$ ms^{-1} and increased again after $U_G = 0.1$ ms^{-1} as superficial gas velocity increased. It suggested the presence of two different zones in the downcomer. Patel et al. [9] observed similar results in their studies of a split-cylinder airlift column. They proposed that the downcomer of the airlift reactor could be divided into two zones and in the upper zone bubble breakage was prevalent while bubble coalescence became dominant further down the column. Previous investigators [2, 20] reported the presence of a vortex in the upper entrance region of the downcomer. The size and strength of this vortex increases as gas velocity increases. As a result of large bubbles in the zone are broken up into smaller bubbles. The increase of bubble size above $U_G = 0.1$ ms^{-1} may be explained that the residence time of gas bubbles in the vortex region decreases with increasing air flow rate.

The bubbles in the downcomer coalesce to form larger bubbles. In contrast to bubble columns, the large bubbles move upward, medium size bubbles are stagnant, while small bubbles are carried down by the circulation liquid. Erickson and Deshpande [13], Wieland [14], and Siegel et al. [15] visually observed that the bubble size reduced towards the lower region of the downcomer. The phenomenon may be vivid for coalescence promoting liquid such as a carboxy-
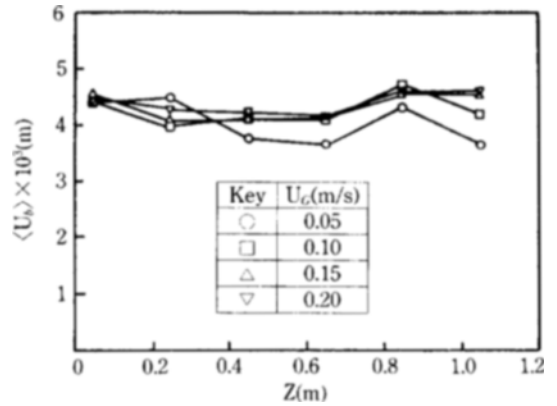

Fig. 11. **Effect of distance from top of draft tube on cross-sectional average of vertical bubble length in down-comer.**
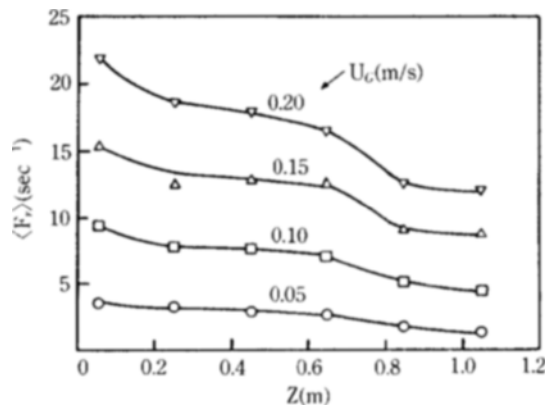

Fig. 12. **Effect of distance from top of draft tube on cross-sectional average of bubble frequency in down-comer.**

methyl cellulose(CMC) solution. For lower superficial gas velocity($U_G = 0.05$ ms^{-1}), the vertical bubble length at $Z = 0.45$ m was smaller than that at $Z = 0.25$ m as shown in Fig. 11. Since the circulation liquid velocity was low, the bubble which coalesced in the lower region of the downcomer occasionally rose up and reached this zone. Then the bubble was broken up into smaller bubbles and again carried downward with the flow. Only one or two bubbles escaped the down-comer via its entrance. The downcomer region becomes increasingly turbulent at higher gas velocities. The coalesced bubble did not reach to the top of the downcomer but it was broke into small bubbles by the liquid turbulent in a few second. At high superficial gas velocity, the vertical bubble length slightly decreased with an increase in Z in the upper region

of the downcomer as shown in Fig. 11. But highest value of the vertical bubble length was observed at $Z = 0.85$ m. It may be due to the periodically generated large bubbles which resulted from the pressure fluctuation in the connection section.

In Fig. 12, the cross-sectionally averaged bubble frequency is plotted against the distance from the upper end of the draft tube in the downcomer. The cross-sectionally averaged bubble frequency is obtained by

$$\langle F_r \rangle = \frac{2\pi}{A} \int_{r_1}^{r_2} F_r \ r \ dr \qquad (5)$$

At first, the bubble frequency steeply decreased due to the presence of a vortex. And the second steep decrease of the bubble frequency results from the presence of the lower zone which bubble coalescence was prevalent.

CONCLUSIONS

The radial distributions of the local gas holdup, bubble size and bubble frequency in the riser and the downcomer were found to be non-uniform. The profiles of the local gas holdup, vertical bubble length and bubble rising velocity in the riser were shown as parabolic shapes.

Two different zones exist in the downcomer. Breakup of bubbles is prevalent in the upper zone and some bubble coalescence takes place in the lower zone.

The vertical bubble length, the bubble rising velocity and the bubble frequency at axis in the riser increased with increasing superficial gas velocity and the bed height. The local gas holdup, the vertical bubble length and the bubble frequency in the downcomer changed with superficial gas velocity and the distance from the top of the draft tube.

NOMENCLATURE

A   : cross-sectional area $[m^2]$
D   : column diameter $[m]$
D_D : inside diameter of draft tube $[m]$
F_r : bubble frequency
H   : bed height $[m]$
i.d. : inside diameter $[m]$
L_v : vertical bubble length $[m]$
m   : constant
n   : constant
n_b : number of bubbles
R   : inside radius of draft tube $[m]$
r   : radial distance from axis $[m]$

R.C. : regression coefficient
r_1 : outer radius of draft tube $[m]$
r_2 : inner radius of main column $[m]$
S.D. : standard deviation
U_b : bubble rising velocity $[m/sec]$
U_G : superficial gas velocity $[m/sec]$
U_L : superficial liquid velocity $[m/sec]$
Z   : distance measured from top of draft tube $[m]$

Greek Letter
ε : local gas holdup

Subscripts
c   : center
w   : wall
$\langle \ \rangle$: cross-sectionally averaged values from integral

REFERENCES

1. Lin, C. H., Fang, B. S., Wu, C. S., Fang, H. Y., Kuo, T. F. and Hu, C. Y.: *Biotechnol. Bioeng.*, **18**, 1557 (1976).
2. Chisti, M. Y. and Moo-Young, M.: *Chem. Eng. Commun.*, **60**, 195 (1987).
3. Mercer, D. G.: *Biotechnol. Bioeng.*, **23**, 2421 (1981).
4. Lippert, J., Adler, I., Meyer, H. D., Lubbert, A. and Schügerl, K.: *Biotechnol. Bioeng.*, **25**, 437 (1983).
5. Koide, K., Kurematsu, K., Iwamoto, S., Iwata, Y. and Horibe, K.: *J. Chem. Eng. Japan*, **16**, 413 (1983).
6. Glasgow, L. A., Erickson, L. E., Lee, C. H. and Patel, S. A.: *Chem. Eng. Commun.*, **29**, 311 (1984).
7. Choi, K. H., Kim, J. W. and Lee, W. K.: *Korean J. Chem. Eng.*, **3**, 127 (1986).
8. Miyahara, T., Hamaguchi, M., Sukeda, Y. and Takahashi, T.: *Can. J. Chem. Eng.*, **64**, 718 (1986).
9. Patel, S. C., Glasgow, L. A., Erickson, L. E. and Lee, C. H.: *Chem. Eng. Commun.*, **44**, 1 (1986).
10. Popovic, M. and Robinson, C. W.: *Chem. Eng. Sci.*, **42**, 2811 (1987).
11. Popovic, M. and Robinson, C. W.: *Chem. Eng. Sci.*, **42**, 2825 (1987).
12. Fan, L. S., Hwang, S. J. and Matsuura, A.: *Chem. Eng. Sci.*, **39**, 1677 (1984).
13. Erickson, L. E. and Deshpande, V.: "Gas-Liquid Dispersion Characteristics in Airlift Fermentors", Pro. 6th Int. Frement. Symp., London, Pergamon Press, 533 (1980).
14. Weiland, P.: *Ger. Chem. Eng.*, 7, 374 (1984).
15. Siegel, M. H., Merchuk, J. C. and Schügerl, K.: *AIChE J.*, **32**, 1585 (1986).
16. Choi, K. H. and Lee, W. K.: *Chem. Eng. Comm.*,

91, 35 (1990).

17. Hills, J. H.: *Trans. Inst. Chem. Engrs.*, **52**, 1 (1974).
18. Serizawa, A., Kataoka, I. and Michiyoshi, I.: *Int. J. Multiphase Flow*, **2**, 235 (1975).
19. Ueyama, K., Morooka, S., Koide, K., Kaji, H. and Miyauchi, T.: *Ind. Eng. Chem. Proc. Des. Dev.*, **19**, 592 (1980).
20. Orazem, M. E., Fan, L. T. and Erickson, L. E.: *Biotechnol. Bioeng.*, **21**, 1579 (1979).